Magnetic resonance imaging reference values for cardiac morphology, function and tissue composition in adolescents

Carlos Real,[a,b] Rocío Párraga,[a,b] Gonzalo Pizarro,[a,c,d] Inés García-Lunar,[a,d,e] Ernesto González-Calvo,[a,b] Jesús Martínez-Gómez,[a] Javier Sánchez-González,[f] Patricia Sampedro,[a] Irene Sanmamed,[a] Mercedes De Miguel,[a,g] Amaya De Cos-Gandoy,[a,g] Patricia Bodega,[a,g] Borja Ibanez,[a,d,h] Gloria Santos-Beneit,[g,i] Valentin Fuster,[a,i] and Rodrigo Fernández-Jiménez[a,b,d,*]

[a]Centro Nacional de Investigaciones Cardiovasculares, Madrid, Spain
[b]Department of Cardiology, Hospital Universitario Clínico San Carlos, Madrid, Spain
[c]Department of Cardiology, Hospital Ruber Juan Bravo Quironsalud UEM, Madrid, Spain
[d]CIBER de enfermedades cardiovasculares (CIBER-CV), Madrid, Spain
[e]Cardiology Department, University Hospital La Moraleja, Madrid, Spain
[f]Philips Healthcare Spain, Madrid, Spain
[g]Foundation for Science, Health and Education (SHE), Barcelona, Spain
[h]Department of Cardiology, Hospital Fundación Jiménez Díaz, Madrid, Spain
[i]The Zena and Michael A. Wiener Cardiovascular Institute, Icahn School of Medicine at Mount Sinai, New York, USA

eClinicalMedicine
2023;57: 101885
Published Online 3 March 2023
https://doi.org/10.1016/j.eclinm.2023.101885

Summary

Background Cardiovascular magnetic resonance (CMR) is a precise tool for the assessment of cardiac anatomy, function, and tissue composition. However, studies providing CMR reference values in adolescence are scarce. We aim to provide sex-specific CMR reference values for biventricular and atrial dimensions and function and myocardial relaxation times in this population.

Methods Adolescents aged 15–18 years with no known cardiovascular disease underwent a non-contrast 3-T CMR scan between March 2021 and October 2021. The imaging protocol included a cine steady-state free-precession sequence for the analysis of chamber size and function, as well as T2-GraSE and native MOLLI T1-mapping for the characterization of myocardial tissue.

Findings CMR scans were performed in 123 adolescents (mean age 16 ± 0.5 years, 52% girls). Mean left and right ventricular end-diastolic indexed volumes were higher in boys than in girls (91.7 ± 11.6 vs 78.1 ± 8.3 ml/m^2, $p < 0.001$; and 101.3 ± 14.1 vs 84.1 ± 10.5 ml/m^2, $p < 0.001$), as was the indexed left ventricular mass (48.5 ± 9.6 vs 36.6 ± 6.0 g/m^2, $p < 0.001$). Left ventricular ejection fraction showed no significant difference by sex (62.2 ± 4.1 vs 62.8 ± 4.2%, $p = 0.412$), whereas right ventricular ejection fraction trended slightly lower in boys (55.4 ± 4.7 vs. 56.8 ± 4.4%, $p = 0.085$). Indexed atrial size and function parameters did not differ significantly between sexes. Global myocardial native T1 relaxation time was lower in boys than in girls (1215 ± 23 vs 1252 ± 28 ms, $p < 0.001$), whereas global myocardial T2 relaxation time did not differ by sex (44.4 ± 2.0 vs 44.1 ± 2.4 ms, $p = 0.384$). Sex-stratified comprehensive percentile tables are provided for most relevant cardiac parameters.

Interpretation This cross-sectional study provides overall and sex-stratified CMR reference values for cardiac dimensions and function, and myocardial tissue properties, in adolescents. This information is useful for clinical practice and may help in the differential diagnosis of cardiac diseases, such as cardiomyopathies and myocarditis, in this population.

Funding Instituto de Salud Carlos III (PI19/01704).

Keywords: Adolescent; Reference values; Magnetic resonance; Pediatrics; Ventricular function; Differential diagnosis

*Corresponding author. Centro Nacional de Investigaciones Cardiovasculares (CNIC). Calle Melchor Fernández Almagro, 3, 28029, Madrid, Spain.
E-mail address: rodrigo.fernandez@cnic.es (R. Fernández-Jiménez).

Research in context

Evidence before this study

Cardiovascular magnetic resonance (CMR) is considered the most accurate non-invasive tool for assessing the morphology and function of the heart. Most studies assessing cardiac structure and function in healthy pediatric populations have used echocardiography. As the use of CMR expands, it is essential to have CMR reference values to define diseased and healthy cardiac states. However, studies providing CMR reference values in adolescence are scarce.

Added value of this study

CMR scans were performed in 123 adolescents (mean age 16 ± 0.5 years, 52% girls). Mean left and right ventricular end-diastolic indexed volumes were higher in boys than in girls (91.7 ± 11.6 vs 78.1 ± 8.3 ml/m^2, p < 0.001; and 101.3 ± 14.1 vs 84.1 ± 10.5 ml/m^2, p < 0.001), as was the indexed left ventricular mass (48.5 ± 9.6 vs 36.6 ± 6.0 g/m^2, p < 0.001). Left ventricular ejection fraction showed no significant difference by sex (62.2 ± 4.1 vs 62.8 ± 4.2%, p = 0.412), whereas right ventricular ejection fraction trended slightly lower in boys (55.4 ± 4.7 vs. 56.8 ± 4.4%, p = 0.085). Indexed atrial size and function parameters did not differ significantly between sexes. Global myocardial native T1 relaxation time was lower in boys than in girls (1215 ± 23 vs 1252 ± 28 ms, p < 0.001), whereas global myocardial T2 relaxation time did not differ by sex (44.4 ± 2.0 vs 44.1 ± 2.4 ms, p = 0.384).

Implications of all the available evidence

This study provides overall and sex-stratified CMR reference values and percentile tables for cardiac dimensions and function, and myocardial tissue properties, in adolescents. This information is useful for clinical practice and may help in the differential diagnosis of cardiac diseases, such as cardiomyopathies and myocarditis, in this population.

Introduction

Cardiovascular magnetic resonance (CMR) is increasingly used as an accurate, reproducible, and radiation-free non-invasive imaging tool for the clinical evaluation of the heart. CMR is established as the reference standard for assessing the dimensions and function of the right ventricle (RV) and the left ventricle (LV) in adult and pediatric populations.[1,2] CMR is also considered the most accurate non-invasive tool for assessing the atrial chambers because of its superior spatial resolution and the excellent contrast it offers between the blood pool and myocardium.[3] Moreover, CMR allows in-vivo myocardial tissue characterization with the use of mapping sequences that are able to quantify subtle changes in myocardial composition, such as edema or fibrosis, based on myocardial T1 and T2 relaxation time properties. These changes can appear in diseases that might affect children and adolescents, such as myocarditis[4] and several cardiomyopathies.[5]

Due to considerations of simplicity and availability, most studies assessing cardiac structure and function in healthy pediatric populations have used echocardiography; however, as the use of CMR expands, it is essential to have CMR reference values to define diseased and healthy cardiac states. Previous studies have provided CMR reference values for biventricular volumes and function[2,6–8] and atrial size and function[9] in pediatric populations, but these studies covered a wide age range encompassing the whole of childhood and adolescence, with small sample sizes in each age subcategory. To our knowledge, no previous study has provided reference values for myocardial T1 and T2 mapping values in adolescence. The aim of the present study was to establish sex-specific CMR reference values for a battery of relevant cardiac parameters in adolescents with no known cardiovascular disease.

Methods

Study population

This study enrolled adolescents aged 15–18 years as part of the *Early ImaginG Markers of unhealthy lifestyles in Adolescents* (EnIGMA) project. For recruitment, the study took advantage of an already running cluster-randomized trial (NCT03504059) that includes 24 public secondary schools in Spain, encompassing 1326 adolescents[10]; a detailed analysis of their cardiovascular health status at enrollment can be found elsewhere.[11] For inclusion, adolescents needed to be enrolled in the cited trial and attend one of the 7 schools in the trial located in the Madrid region as of December 2020. Exclusion criteria were general contraindications for a CMR examination (pacemakers, cochlear implants, known claustrophobia, etc.), pregnancy, and evidence or history of cardiovascular disease.

All adolescents meeting the inclusion criteria were invited to participate through printed and email invitation letters sent to them and their parents or caregivers. Those who showed interest were invited to virtual meetings in which the study was presented and questions answered by investigators and clinicians leading the study. Invitees who verbally agreed to participate were scheduled to attend the imaging facilities at the *Centro Nacional de Investigaciones Cardiovasculares* (CNIC), where informed consent was signed and the CMR scan performed. The reporting of this study adheres to the *Strengthening The Reporting of Observational studies in Epidemiology* (STROBE) guideline for cross-sectional studies.[12]

Ethics statement

Written informed consent was obtained from all participants and at least one parent or caregiver. The study protocol was approved by the research ethics committee of the *Instituto de Salud Carlos III* in Madrid, under identifier CEI PI 63_2020.

CMR acquisition protocol

CMR examinations were conducted between March-2021 and October-2021 using a Philips 3-T Elition X whole-body scanner (Philips Healthcare, Best, The Netherlands) equipped with a 28-element phased-array Torso-Cardiac coil. Body weight and height were measured immediately before the CMR examination. The cardiac imaging protocol included a standard segmented cine steady-state free-precession (SSFP) sequence to provide high-quality images for the assessment of cardiac chamber dimensions and function, as well as a mid-ventricular T2 gradient-spin-echo (T2-GraSE) mapping sequence[13] and a mid-ventricular 5 (3)3 modified look-locker inversion recovery (MOLLI) T1 mapping sequence for myocardial tissue characterization. Participant heart rate was recorded during SSFP CMR acquisition. The imaging protocol did not include administration of intravenous gadolinium contrast. Technical details of image acquisition are detailed in the Supplementary Appendix.

CMR analysis

Images were analyzed by experienced observers using a dedicated software program available at the CNIC imaging core lab (IntelliSpace Portal v12.1, Haifa, Israel). For the indexing of CMR values, body surface area (BSA) was determined with the Du Bois formula. Body mass index (BMI) was calculated as weight (kg) divided by height squared (m^2). Age- and sex-adjusted BMI z-scores and percentiles were calculated based on Centers for Disease Control reference values.[14] According to these BMI percentiles, participants were categorized as being of normal weight (<P85), overweight (P85–P95), or obese (>P95).

Cardiac cine imaging – ventricular volumes and function

LV endocardial and epicardial borders were manually traced in the end-diastolic phase, whereas only LV endocardial borders were traced in the end-systolic phase (Fig. 1). RV endocardial borders were manually traced in the end-diastolic and end-systolic phases (Fig. 1). Ventricular volume was calculated using the Simpson method. For the purpose of analysis, papillary muscles were included as part of the LV cavity volume. LV myocardial volume was calculated as the difference between the epicardial and endocardial volumes at the end-diastolic phase, and LV mass was computed as the myocardial volume multiplied by myocardial density (1.05 g/ml). The LV end-diastole and end-systole phases were visually defined based on short and long axis images (of the maximum and minimum volume, respectively), and the defined phases were assigned to both ventricles.

LV contours in the basal slices were included if > 50% of the cavity was bounded by myocardium. If myocardium with trabeculations was visible in basal slices, these were considered part of the RV rather than the right atrium or pulmonary artery. In uncertain cases, the identification of basal slices was facilitated by simultaneous visualization in long axis views. The LV and RV outflow tracts were considered part of the ventricles and were therefore included in the corresponding ventricular volume. The interventricular septum was included in the LV mass.

Strokes volumes (SV) were obtained as end-diastolic volume (EDV) – end-systolic volume (ESV). LV and RV ejection fraction (LVEF, RVEF) were computed as EF (%) = (EDV - ESV)/EDV. LVEDV, RVEDV, LVESV, RVESV, LVSV, RVSV, and LV mass were normalized to BSA.

Cardiac cine imaging – atrial size and function

For the left atrium (LA), volumes were measured using the biplane area–length method with 4-chamber (4Ch) and 2-chamber (2Ch) views,[15] whereas for the right atrium (RA) only area and length were reported because the RA could be assessed only in 4Ch view (Fig. 2).

The atrial endocardial border was manually traced to determine LA area with exclusion of the pulmonary veins, LA appendage (LAA), and mitral valve recess.[16] The anterior border of the LA was thus at the mitral annular plane, and the posterior border was at the pulmonary vein ostia. The RA endocardial border was manually traced with exclusion of the superior and inferior vena cava and the RA appendage. The anterior border of the RA was thus placed at the tricuspid annular plane.

Maximum LA volume (LAV) was obtained in the frame immediately before mitral valve opening, and minimum LAV was obtained in the frame immediately after mitral valve closure. LA pre-atrial contraction volume was obtained in the frame immediately before atrial contraction.

LAVs were calculated offline with statistical software using the area–length method (volume = [0.85 × 2Ch area x 4Ch area]/length). Calculations were made with the shorter length between 2Ch and 4Ch views.

Atrial function was considered in three phases: reservoir (pulmonary venous return storage during LV contraction and isovolumetric relaxation), conduit (passive blood transfer into the LV), and pump (active contraction during the final diastolic phase). The following formulas were used for calculation of atrial function parameters:[16]

*LA emptying fraction (LAEF) (reservoir function): [(LAVmax - LAVmin)/LAVmax] × 100.

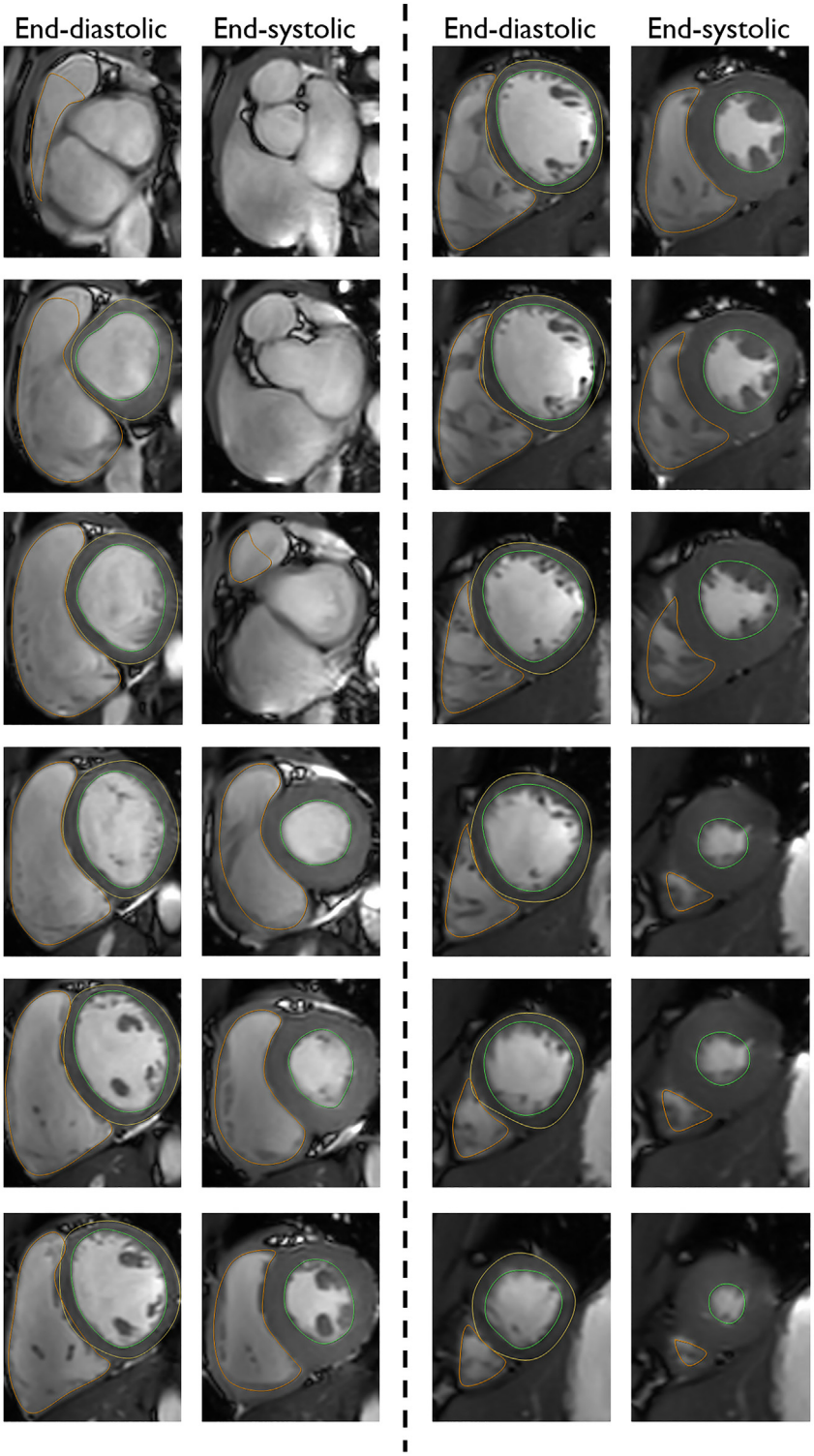

Fig. 1: **Ventricular tracing in cardiovascular magnetic resonance cine sequences**. Ventricular slices and tracing from base (top left) to apex (bottom right) of the same participant during the end-diastolic and end-systolic phases of the cardiac cycle.

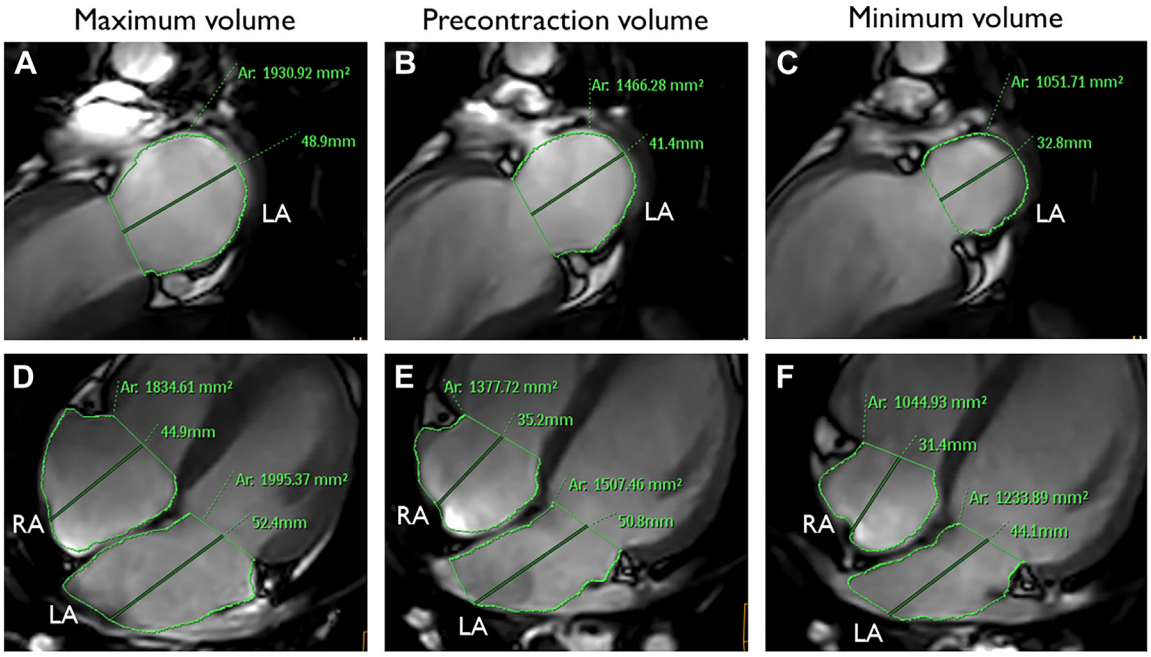

***Fig. 2:* Atrial tracing in cardiovascular magnetic resonance cine sequences**. Representative 2-chamber (A, B, C) and 4-chamber (D, E, F) long-axis views. For the calculation of atrial function, the left atrium (LA) and right atrium (RA) were assessed in the maximum-volume, pre-contraction-volume, and minimum-volume phases.

*LA passive emptying fraction (LAPEF) (conduit function): [(LAVmax - LAVprec)/LAVmax] × 100.

*LA active emptying fraction (LAAEF) (pump function): [(LAVprec - LAVmin)/LAVprec] × 100.

Parametric myocardial mapping

The LV endocardial and epicardial borders were manually traced by an experienced observer, ensuring that no blood or epicardial fat was included in the region of interest (ROI). The myocardial ROI was automatically segmented according to the American Heart Association (AHA) segment model,[17] thus obtaining 6 segments in the mid-ventricular slice (Fig. 3).

Images were assessed for susceptibility effects and for cardiac or respiratory motion, and a motion correction tool was used when needed. The presence of artifacts despite motion correction led to the exclusion of the affected myocardial segment. For each participant, global averaged myocardial relaxation time was obtained as the area weighted mean value of all analyzable segments. If more than two segments were of poor quality, the whole corresponding mapping study was excluded from analysis. Global and septum values are reported, as recommended by the Society for Cardiovascular Magnetic Resonance (SCMR) for global assessment in both T1 and T2 mapping.[18]

Statistical analysis

Study data were collected and managed using the REDCap electronic data capture tool hosted at the CNIC. Normal distribution assumptions were verified with the use of box plots, normal probability plots and density function histograms; thus, normal distribution was the case for the majority of variables analyzed. Continuous variables are presented as means ± one standard deviation (SD), and categorical variables are presented as frequencies and percentages, unless otherwise specified. The Student t-test was used for between-sex comparisons of continuous variables, while the chi-square test was used for comparisons of categorical variables. For comparisons of continuous variables not following a normal distribution, analysis was supplemented with the use of the Wilcoxon (Mann–Whitney) test. Sex-specific percentiles were calculated using the weighted average method.

Intraobserver and interobserver agreement was assessed in 30 randomly selected participant studies and reanalyzed with the use of intraclass correlation coefficients (ICC) and Bland–Altman plots. ICC values and their 95% confidence intervals (CI) were calculated using the *icc* command for two-way random-effects model. Agreement was considered poor, moderate, good, or excellent for ICC <0.50, 0.50 to 0.75, 0.75 to 0.90, and >0.90, respectively. For Bland–Altman analysis, no significant systematic bias was assumed if the

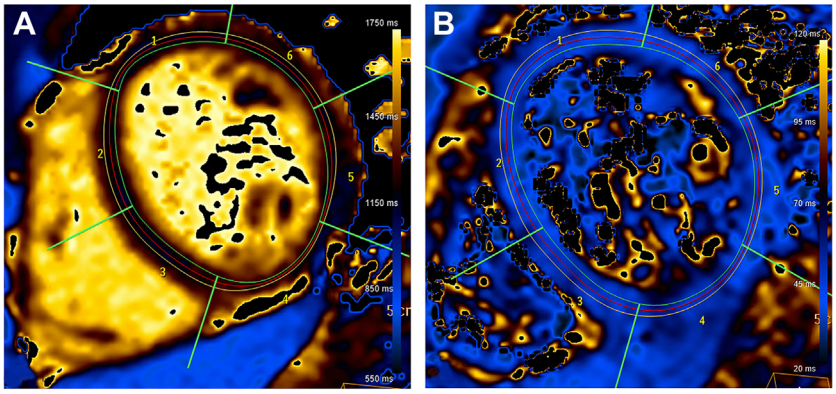

Fig. 3: **Parametric mapping manual contouring**. Representative T1 (A) and T2 (B) mapping assessed in a mid-ventricular slice from the same participant. The myocardium was divided into 6 segments according to the American Heart Association (AHA) segment model, indicated by the following numbers: 1 (mid anterior), 2 (mid anteroseptal), 3 (mid inferoseptal), 4 (mid inferior), 5 (mid inferolateral), and 6 (mid anterolateral).

95% confidence interval (CI) for the mean between-measurement difference contained the value 0.

All statistical analyses were performed with Stata software package version 16 (StataCorp, College Station, Texas).

Role of the funding source

The funding sources had no role in study design; in the collection, analysis, and interpretation of data; in the writing of the report; and in the decision to submit the paper for publication. All authors confirm that they had full access to all the data in the study and accept responsibility to submit for publication.

Results

General characteristics

A total of 345 adolescents met the inclusion criteria and were invited to participate through printed and email invitation letters sent to them and their parents/caregivers (Fig. 4). Approximately 43% of them responded to the invitation. Among 124 participants who finally gave written informed consent, one was unable to undergo the CMR examination due to claustrophobia. The analysis thus included 123 participants (overall response rate ~36%), with a mean age of 16 ± 0.5 years, of whom 52% were girls. 117 participants (95%) were born in Spain, while 5 (4%) were born in Latin America and 1 (1%) was born in Africa; within the 117 adolescents born in Spain, 26 (22%) had a migrant background (at least one parent/caregiver born outside Spain). General participant characteristics are listed in Table 1. Boys had higher weight, height, and body surface area (BSA) than girls, whereas there were no between-sex differences in mean BMI or in-scan heart rate. Nevertheless, a higher percentage of girls were of normal weight according to categorized BMI percentiles.

Cardiac chamber dimensions and function

Descriptive summary statistics of the most important cine-imaging-derived clinical parameters are shown in Table 2. None of the imaging studies showed signs of significant structural heart disease. Boys had larger indexed biventricular volumes and LV mass (48.5 ± 9.6 vs 36.6 ± 6.0 g/m^2, $p < 0.001$). LVEF was similar in both sexes (62.2 ± 4.1 vs. 62.8 ± 4.2%, $p = 0.412$), whereas RVEF trended higher in girls than in boys (56.8 ± 4.4% vs. 55.4 ± 4.7 vs, $p = 0.085$). Indexed LA volumes and RA area, as well as LA function measurements, were similar in boys and girls. Sex-stratified reference values for these CMR parameters, in the form of user-friendly clinically relevant percentiles, are provided in Table 3. Non-indexed ventricular parameters are included in Supplementary Table S1, and the remaining atrial parameters are provided in Supplementary Table S2. Intraobserver and interobserver agreement was good for most of the parameters analyzed (Supplementary Table S3 and S4 and Supplementary Figs. S1 and S2).

Non-invasive myocardial tissue characterization

A total of 4 T1-mapping studies and 5 T2-mapping studies were excluded in their entirety due to poor image quality in more than 2 mid-ventricular segments. In the remaining participants, 699 out of 714 segments (98%) were eligible for T1-mapping analysis, and 701 out of 708 segments (99%) were eligible for T2-mapping analysis. The majority of the excluded segments (78%) were located in the inferior/inferolateral wall and were mostly related to susceptibility artifacts.

Myocardial T1 relaxation times were higher in girls than in boys, both when measured as the mean of the global myocardial LV values (1252 ± 28 ms vs 1215 ± 23 ms, $p < 0.001$) and when comparing only values in the septal segments (1261 ± 31 ms vs 1220 ± 26 ms, $p < 0.001$) (Table 4). We found no between-sex differences in global T2 relaxation time;

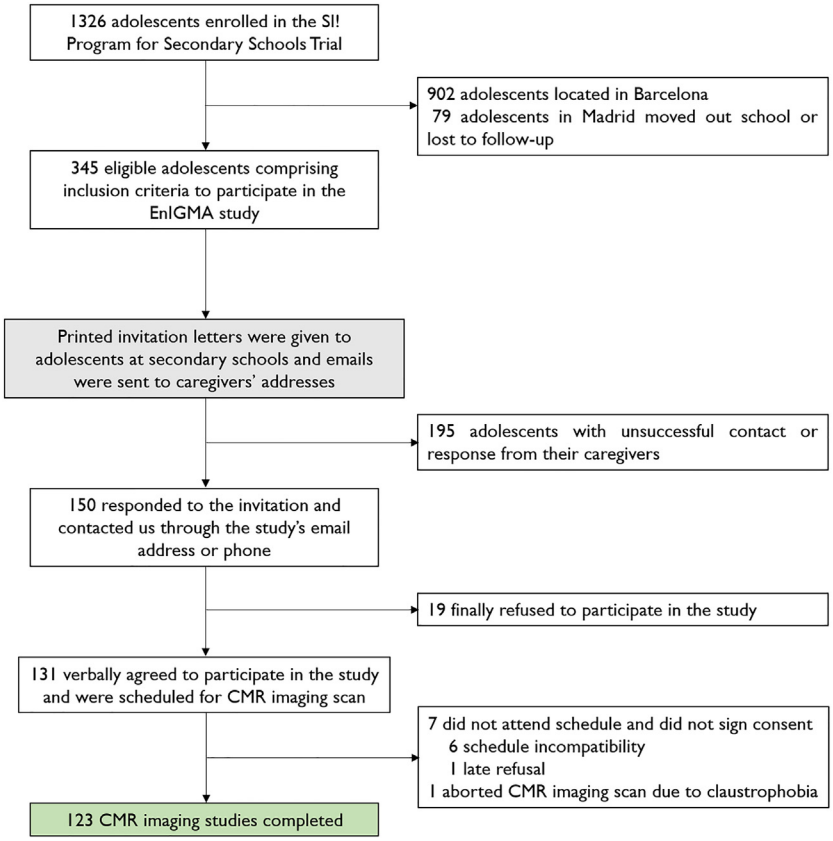

***Fig. 4:* Flow diagram of participants**. CMR, cardiovascular magnetic resonance; EnIGMA, Early ImaGing Markers of unhealthy lifestyles in Adolescents.

	Overall	Boys	Girls	p-value
	N = 123 (100%)	n = 59 (48%)	n = 64 (52%)	
Age, years	16.0 (0.4)	16.1 (0.5)	16.0 (0.4)	0.384
Weight, kg	61.0 (10.5)	65.1 (10.1)	57.2 (9.4)	<0.001
Height, m	1.69 (0.09)	1.75 (0.07)	1.63 (0.06)	<0.001
BMI, kg/m^2	21.4 (3.2)	21.3 (2.9)	21.5 (3.5)	0.698
BMI z-score	0.09 (0.89)	0.04 (0.97)	0.13 (0.82)	0.586
Categorized BMI				0.005
Normal weight	107 (87.0%)	47 (79.7%)	60 (93.8%)	
Overweight	12 (9.8%)	11 (18.6%)	1 (1.6%)	
Obesity	4 (3.3%)	1 (1.7%)	3 (4.7%)	
Body surface area, m^2	1.69 (0.16)	1.79 (0.15)	1.61 (0.12)	<0.001
Heart rate, bpm	69 (11)	68 (11)	69 (11)	0.663

Data are shown as mean (SD) for continuous variables and n (%) for categorical variables. P-values denote the significance of between-sex differences for continuous variables analyzed by the Student t-test. The significance of sex-differences for categorical variables was tested by the chi-square test. BMI categories were defined according to age- and sex-adjusted body mass index percentiles (P) based on Centers for Disease Control reference values: normal weight (<P85), overweight (P85–P95), and obese (>P95). BMI, body mass index.

***Table 1:* Participant characteristics, overall and stratified by sex.**

however, T2 relaxation time in the mid-ventricular septal segments was slightly higher in boys than in girls (45.6 ± 2.8 ms vs 44.0 ± 2.7 ms, p = 0.003) (Table 4). Sex-stratified percentile values for parametric mapping parameters are provided in a user-friendly format for clinical use in Table 5. Intraobserver and interobserver

	Overall	Boys	Girls	p-value
	N = 123 (100%)	n = 59 (48%)	n = 64 (52%)	
LVEDVi, ml/m^2	84.6 (12.1)	91.7 (11.6)	78.1 (8.3)	<0.001
LVESVi, ml/m^2	31.9 (6.4)	34.8 (6.6)	29.1 (4.8)	<0.001
iLVmass, g/m^2	42.3 (9.9)	48.5 (9.6)	36.6 (6.0)	<0.001
LVEF, %	62.5 (4.1)	62.2 (4.1)	62.8 (4.2)	0.412
LVSVi, ml/m^2	52.8 (7.5)	56.6 (7.1)	49.0 (5.8)	<0.001
RVEDVi, ml/m^2	92.4 (15.0)	101.3 (14.1)	84.1 (10.5)	<0.001
RVESVi, ml/m^2	40.8 (9.3)	45.4 (9.2)	36.6 (7.2)	<0.001
RVEF, %	56.2 (4.6)	55.4 (4.7)	56.8 (4.4)	0.085
RVSVi, ml/m^2	51.6 (7.6)	55.9 (7.5)	47.6 (5.0)	<0.001
iLAVmax, ml/m^2	37.8 (7.3)	39.1 (7.7)	36.7 (6.8)	0.070
iLAVprec, ml/m^2	21.8 (5.9)	22.5 (6.3)	21.1 (5.4)	0.169
iLAVmin, ml/m^2	14.3 (4.2)	14.7 (4.5)	14.0 (4.0)	0.325
LAEF, %	62.3 (7.8)	62.5 (8.3)	62.1 (7.4)	0.797
LAPEF, %	42.9 (8.3)	42.9 (9.0)	43.0 (7.7)	0.986
LAAEF, %	33.9 (10.0)	34.4 (9.9)	33.5 (10.3)	0.596
iRAAmax, cm^2/m^2	11.1 (1.5)	11.3 (1.6)	11.0 (1.4)	0.279

Indexed cardiac dimensions and function parameters are shown, overall and stratified by sex. Data are shown as mean (SD). p-values are derived from the analysis of between-sex differences by the Student t-test. For those continuous variables not following a normal distribution (i.e., RVEF), the p-value from the analysis of between-sex differences as analyzed by the Wilcoxon (Mann–Whitney) was 0.041. LVEDV, left ventricular end-diastolic volume; LVESV, left ventricular end-systolic volume; LVEF, left ventricular ejection fraction; LVSV, left ventricular stroke volume; RVEDV, right ventricular end-diastolic volume; RVESV, right ventricular end-systolic volume; RVEF, right ventricular ejection fraction; RVSV, right ventricular stroke volume; LAVmax, left atrial maximum volume; LAVprec, left atrial pre-contraction volume; LAVmin, left atrial minimum volume; LAEF, left atrial emptying fraction; LAPEF, left atrial passive emptying fraction; LAAEF, left atrial active emptying fraction; RAAmax, right atrial maximum area; i, indexed to body surface area.

Table 2: **Biventricular and atrial cardiovascular magnetic resonance imaging values, overall and stratified by sex.**

	BOYS							GIRLS						
	P3	P10	P25	P50	P75	P90	P97	P3	P10	P25	P50	P75	P90	P97
LVEDVi, ml/m^2	74.3	76.6	82.2	90.3	99.9	108.0	117.7	61.2	67.6	72.7	78.5	82.7	88.2	97.2
LVESVi, ml/m^2	24.3	27.3	28.7	34.1	39.5	43.2	49.5	19.6	22.4	25.7	29.6	32.3	35.8	38.7
iLVmass, g/m^2	34.3	36.8	40.1	47.9	55.1	60.7	70.9	26.6	30.7	32.4	35.7	39.0	46.7	49.0
LVEF, %	53.6	56.8	59.8	61.7	65.6	67.9	69.7	54.7	56.3	60.0	62.6	66.4	68.6	70.6
LVSVi, ml/m^2	46.2	49.5	52.4	54.8	61.7	66.0	74.6	40.0	41.4	45.1	48.5	51.6	57.4	63.3
RVEDVi, ml/m^2	75.5	86.0	90.6	99.7	110.8	122.1	129.6	59.9	72.6	78.7	83.9	89.7	95.3	102.1
RVESVi, ml/m^2	30.4	34.0	38.2	45.2	53.7	57.7	63.5	20.1	26.9	33.1	37.0	40.7	44.1	49.9
RVEF, %	47.5	49.2	51.3	55.4	58.2	62.7	65.7	48.1	51.2	53.7	57.1	58.8	62.9	66.4
RVSVi, ml/m^2	42.2	46.9	50.2	55.8	60.5	67.7	72.0	36.7	40.6	44.6	47.6	50.5	54.8	58.1
iLAVmax, ml/m^2	25.5	29.2	33.4	37.8	43.8	51.6	54.2	24.5	29.1	32.5	35.9	40.8	47.8	51.8
iLAVprec, ml/m^2	10.7	12.7	18.2	22.4	26.9	31.0	34.8	12.9	14.0	16.4	20.8	25.1	27.5	35.7
iLAVmin, ml/m^2	5.4	8.7	12.5	14.5	17.5	20.6	26.3	7.2	8.7	10.9	14.2	16.5	18.2	25.6
LAEF, %	43.7	52.5	57.7	63.0	68.0	71.1	82.0	44.9	51.6	56.6	63.5	67.6	70.8	76.0
LAPEF, %	25.1	32.2	36.5	42.2	48.7	56.3	61.4	29.6	32.6	37.0	42.2	48.2	54.0	57.0
LAAEF, %	11.3	22.4	29.0	34.4	40.6	47.3	55.5	12.3	16.8	27.3	33.6	40.2	45.9	52.8
iRAAmax, cm^2/m^2	8.2	9.2	10.2	11.2	12.1	13.5	15.5	7.9	8.9	9.8	11.1	12.1	12.9	13.6

Cardiovascular magnetic resonance cine imaging-derived reference values in adolescents for indexed cardiac dimensions and function parameters. LVEDV, left ventricular end-diastolic volume; LVESV, left ventricular end-systolic volume; LVEF, left ventricular ejection fraction; LVSV, left ventricular stroke volume; RVEDV, right ventricular end-diastolic volume; RVESV, right ventricular end-systolic volume; RVEF, right ventricular ejection fraction; RVSV, right ventricular stroke volume; LAVmax, left atrial maximum volume; LAVprec, left atrial pre-contraction volume; LAVmin, left atrial minimum volume; LAEF, left atrial emptying fraction; LAPEF, left atrial passive emptying fraction; LAAEF, left atrial active emptying fraction; RAAmax, right atrial maximum area; i, indexed to body surface area.

Table 3: **Biventricular and atrial cardiovascular magnetic resonance cine imaging reference percentiles in adolescents.**

	Overall	Boys	Girls	p-value
Native T1 relaxation time, ms	**N = 119 (100%)**	**n = 58 (49%)**	**n = 61 (51%)**	
Global	1234 (32)	1215 (23)	1252 (28)	<0.001
Septal	1241 (35)	1220 (26)	1261 (31)	<0.001
T2 relaxation time, ms	**N = 118 (100%)**	**n = 57 (48%)**	**n = 61 (52%)**	
Global	44.2 (2.2)	44.4 (2.0)	44.1 (2.4)	0.384
Septal	44.8 (2.9)	45.6 (2.8)	44.0 (2.7)	0.003

The table shows global values (including all 6 mid-ventricular segments) and isolated septal values (including the 2 septal segments). Data are shown as (SD). p-values are derived from Student t-test of between-sex differences. For those continuous variables not following a normal distribution (i.e., global and septal T2 relaxation time), the p-values from the analysis of between-sex differences as analyzed by the Wilcoxon (Mann–Whitney) were 0.169 and 0.002, respectively.

Table 4: **Myocardial native T1 and T2 relaxation time values, overall and stratified by sex.**

	BOYS							GIRLS						
Native T1 relaxation time, ms	**P3**	**P10**	**P25**	**P50**	**P75**	**P90**	**P97**	**P3**	**P10**	**P25**	**P50**	**P75**	**P90**	**P97**
Global	1176	1189	1197	1214	1230	1250	1267	1206	1218	1233	1247	1270	1292	1309
Septal	1181	1190	1202	1215	1235	1257	1287	1209	1225	1238	1259	1280	1300	1342
T2 relaxation time, ms	**P3**	**P10**	**P25**	**P50**	**P75**	**P90**	**P97**	**P3**	**P10**	**P25**	**P50**	**P75**	**P90**	**P97**
Global	41.2	41.8	42.8	44.1	46.0	47.2	48.8	40.8	41.7	42.7	43.6	44.9	46.7	53.0
Septal	41.5	42.2	43.4	45.3	47.7	49.8	51.7	40.3	41.0	42.4	43.8	45.3	46.8	52.6

Cardiovascular magnetic resonance imaging-derived reference values in adolescents for myocardial native T1 and T2 relaxation time. The table shows global values (including all 6 mid-ventricular segments) and isolated septal values (including the 2 septal segments). P, percentile.

Table 5: **Myocardial native T1 and T2 cardiovascular magnetic resonance mapping reference percentiles in adolescents.**

agreement was good for the mapping parameters analyzed (Supplementary Table S5 and S6 and Supplementary Fig. S3).

Discussion

This study examined a battery of CMR imaging parameters obtained with a state-of-the-art 3-T CMR scanner from a sample of adolescents with no known cardiovascular disease. To our knowledge, this the first study focused on adolescents to provide CMR-imaging-derived reference values for biventricular and atrial dimensions and function, as well as for myocardial tissue characterization parameters (Fig. 5). CMR imaging is central to the diagnosis of cardiac diseases that can appear in adolescent populations, such as cardiomyopathies and myocarditis.[19] In this regard, recently updated Lake-Louis criteria highlight the importance of performing parametric mapping CMR sequences for the detection of myocardial inflammation[4] and the need for CMR reference values to distinguish between the diseased and healthy cardiac states. Furthermore, reference values in younger populations would help to fill the gap in knowledge about the normal physiologic changes from childhood to adulthood.

Our study was performed using a 3-T scanner, whereas reference values for cardiac chamber size and function reported in earlier studies of pediatric populations were mostly obtained with 1.5-T scanners.[2,6–8] The higher spatial and temporal resolution and shorter acquisition time with 3-T CMR may make it more suitable for the study of the relatively smaller hearts and higher heart rates of children and adolescents; however, a potential drawback is that 3-T CMR can be prone to susceptibility artifacts.[20] In the present study, very few cases were excluded because of poor image quality or other technical issues, supporting the feasibility of comprehensive high-quality 3-T CMR studies in adolescent populations.

Van der Ben et al.[2] reported reference values for biventricular volumes and function using pooled data from 3 studies of a total of 141 children and adolescents aged 0–18 years who were examined with a 1.5 T CMR scanner.[6–8] This population included 76 participants between the ages of 12 and 18 years (40 girls and 36 boys), which is the age range closest to that examined in our study. Their analysis revealed higher LV and RV volumes and higher LV mass in boys, in agreement with our findings. The study found no sex-related differences in LVEF or RVEF in this age range. Although we also found no sex-differences in LVEF, in our older adolescent population of 15–18-year-olds, we did find small differences in RVEF, which trended higher in girls than in boys. This between-sex difference is in line with findings in adults,[21] suggesting that differences in RVEF may become evident in the later stage of adolescence or young adulthood.

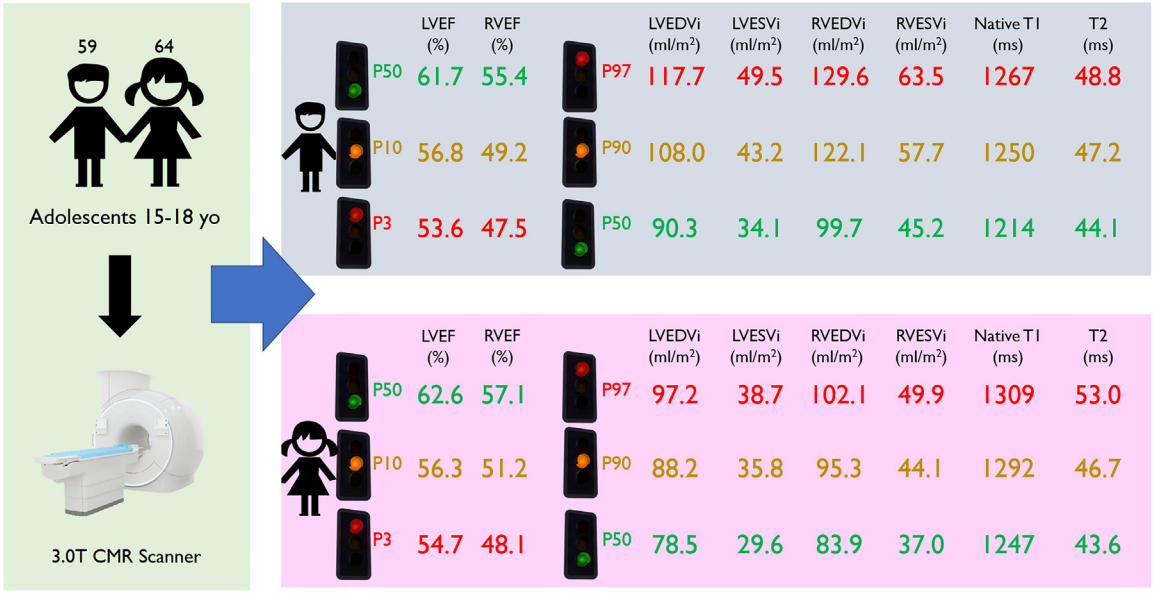

***Fig. 5:* Cardiovascular magnetic resonance reference values in adolescents**. Cardiovascular magnetic resonance (CMR) parameters were obtained from 123 adolescents aged from 15 to 18 years in order to obtain reference values for this population. Median values are shown in green for all parameters displayed. For LVEF and RVEF, P10 and P3 values are shown in yellow and red, respectively. For LVEDVi, LVESVi, RVEDVi, RVESVi, native T1 and T2 mapping, P90 and P97 values are shown in yellow and red, respectively. CMR, cardiovascular magnetic resonance; LVEF, left ventricular ejection fraction; RVEF, right ventricular ejection fraction; LVEDVi, indexed left ventricular end-diastolic volume; LVESVi, indexed left ventricular end-systolic volume; RVEDVi, indexed right ventricular end-diastolic volume; RVESVi, indexed right ventricular end-systolic volume; i, indexed to body surface area; P, percentile.

Compared with the *Van der Ben* et al. study in a mixed-age pediatric population,[2] we found higher overall values for all indexed volumetric ventricular parameters analyzed and slightly lower values for RVEF, LVEF, and LV mass. These differences may be due to the fact that, unlike *Van der Ben* et al.,[2] we excluded papillary muscles and trabecular tissue from the endocardial tracings. RV mass was not measured in our study because we considered that there was insufficient spatial resolution to trace the RV wall in our adolescent population. The difficulty of tracing the thinner RV wall is demonstrated by the modest interobserver agreement for RV mass measurements in the *Van der Ben* et al. study.[2]

Interestingly, our study showed slightly higher both non-indexed and indexed biventricular volumes as compared with adult population studies using similar analysis methods (papillary muscles included as part of the ventricle cavity volume).[22] Nevertheless, LV and RV volume values obtained are comparable to the ones showed for individuals aged 16–20 years old subgroup in a prior study.[23] This finding is in agreement with this study and others, showing that biventricular volumes are higher during late adolescence and young adulthood and decrease with advancing age in both genders.[21,23–25]

The atrium plays a critical role in modulating ventricular filling by functioning as a *reservoir* for venous return during ventricular systole, a *conduit* for venous return during early ventricular diastole, and a *booster pump* that completes ventricular filling during the end-diastolic phase.[26] We observed higher values of LA conduit (passive) function and lower values of LA booster (active) function than those reported in adult CMR studies.[27,28] These findings are consistent with pediatric echocardiography studies, which show conduit-function values peaking between the ages of 5 and 10 years, followed by a progressive decline into adolescence and adulthood, whereas the opposite pattern is observed for booster function.[29] Since atrial function is related to LV compliance, these age-related variations could serve as an early marker of physiological cardiac aging.

Diastolic dysfunction is a characteristic feature of different types of congenital or hereditary heart disease, such as tetralogy of Fallot and hypertrophic cardiomyopathy.[30] Atrial size is related to diastolic dysfunction, whereas atrial function may be affected earlier and is a more sensitive parameter. In patients with congenital heart disease, atrial dysfunction initially affects reservoir and conduit function—triggering a compensatory increase in pump function—and thus eventually affects all three phases.[31] Because CMR provides better image quality and easier border tracking than echocardiography, it is a promising technique for the assessment of atrial function. However, very few studies have assessed

LA and RA volumes and function in healthy children. In one previous publication,[9] atrial volume was measured from short axis images using the Simpson method and included the LAA. Since atrial short axis images are frequently unavailable in routine acquisitions and the bi-plane area-length method in long axis view shows close agreement with the Simpson methods in short axis view,[15] we used 2-chamber and 4-chamber long-axis planes to measure atrial volumes and function. Moreover, the LAA is increasingly excluded from atrial measures,[22] and we therefore consider that our results could easily be applicable in daily clinical practice.

T1 and T2 mapping CMR techniques allow non-invasive myocardial tissue characterization based on quantifiable changes in magnetic tissue properties, i.e. myocardial relaxation time. Diseases that primarily affect the myocardium alter relaxation times, including myocarditis.[4] However, T1 and T2 relaxation times can also be affected by external factors, such as field strength and acquisition scheme.[22] In the present study, we used a MOLLI 5 (3)3 scheme for T1 mapping and a GraSE scheme for T2 mapping. These acquisition schemes are widely used because of their robustness and precision, and are recommended in clinical practice guidelines.[5]

Although there are no published mapping reference values in pediatric populations, a recent meta-analysis[32] revealed a mean myocardial native T1 relaxation time of 1122 ms (95% CI, 1100–1143 ms) in adults who underwent a CMR examination with a Philips 3-T scanner and a MOLLI acquisition scheme. The adolescents scanned in the present study with the same scanner vendor and field strength showed higher native T1 values (1234 ms ± 31.5 ms [mean ± standard deviation]). These differences need to be interpreted with caution, because T1 relaxation time can be significantly influenced by additional factors, such as changes to image acquisition schemes.[33] Intriguingly, girls had slightly higher myocardial native T1 values than boys. This is in line with previous evidence from adults, which showed higher native T1 values in healthy women younger than 45 years.[34] The reason for these sex differences in native T1 relaxation times is unknown.

Reference T2 mapping values are based on relatively small studies, and therefore the effects of age and sex are even less well established.[22] Previous studies in healthy adults revealed an absence of between-sex differences in myocardial T2 values,[35] consistent with our finding of clinically irrelevant differences limited to the mid-ventricular septal segments. Nevertheless, studies done with the same vendor and similar acquisition schemes have reported different T2 values in healthy adult populations,[35] and absolute reference values should therefore be considered indicative.

This study reports reference values of CMR parameters based in a relatively large adolescent sample based in Spain and has some limitations. The impact of race/ethnicity on CMR reference values could not be assessed and the geographical limitation of the sample could compromise external validity. A sensitivity analysis was conducted using mixed models and including school as random effect, and showed very similar results (Supplementary Table S7 and S8). Although the reference mapping values provided should be checked locally by each center, the reported normal ranges make an important contribution to the standardization in CMR imaging.

In conclusion, this study provides overall and sex-stratified 3-T CMR reference values for cardiac-chamber dimensions and function and myocardial tissue properties in adolescents. This information is useful for clinical practice and may help to distinguish between the diseased and healthy cardiac states and in the differential diagnosis of cardiac diseases, such as cardiomyopathies and myocarditis, in adolescent populations.

Contributors

RF-J, JS-G, BI and VF conceived the overall study and provided scientific support over the course of this work. CR and RP coordinated recruitment of participants, the consent process, and data collection for this study. MdM, AdC-G, PB and GS-B coordinated recruitment of schools and participants in the original trial and assisted the recruitment process for the present study. RF-J and JS-G designed the imaging protocol. PS and IS conducted imaging acquisitions. CR, RP, EG-C and RF-J supervised imaging acquisitions and performed initial quality assessment of images for analyses. GP and IG-L performed imaging analyses. CR and JM-G conducted statistical analyses. CR drafted the first version of the manuscript. CR, JM-G and RF-J directly accessed and verified the underlying data reported in the manuscript. All authors revised the manuscript critically for intellectual content and approved the published version.

Data sharing statement

The availability of data collected for the study to external researchers, including data dictionary and deidentified participant data, is restricted to related project proposals upon request to the corresponding author. Based on these premises, data will be available with publication after approval of the proposal and a signed data access/sharing agreement.

Declaration of interests

Javier Sánchez-González is a Philips Healthcare employee. Carlos Real is funded by the *Fundacion Interhospitalaria para la Investigación Cardiovascular*. The remaining authors declare no conflicts of interest.

Acknowledgments

The authors are indebted to the adolescents who participated in this study. Rodrigo Fernández-Jiménez is recipient of grant PI19/01704 by the *Instituto de Salud Carlos III* (ISCIII) - *Fondo de Investigación Sanitaria* and the European Regional Development Fund/European Social Fund (A way to make Europe/Investing in your future), which funded the EnIGMA (Early ImaGing Markers of unhealthy lifestyles in Adolescents) study. Jesús Martínez-Gómez was a postgraduate fellow of the *Ministerio de Ciencia e Innovación* at the *Residencia de Estudiantes* (2020–2022) and is a recipient of grant FPU21/04891 (*Ayudas para la formación de profesorado universitario*, FPU-2021) from the *Ministerio de Educación, Cultura y Deporte* Gloria Santos-Beneit is recipient of grant LCF/PR/MS19/12220001 funded by ""la Caixa" Foundation (ID 100010434). The SHE Foundation is supported by "la Caixa" Foundation (LCF/PR/CE16/10700001). The CNIC is supported by the ISCIII, the *Ministerio de Ciencia e Innovación* (MCIN) and the Pro CNIC Foundation and is a Severo Ochoa Center of Excellence (grant CEX2020-001041-S funded by MICIN/AEI/10.13039/501100011033). Simon Bartlett (CNIC) provided English editing.

Appendix A. Supplementary data

Supplementary data related to this article can be found at https://doi.org/10.1016/j.eclinm.2023.101885.

References

1 Le Ven F, Bibeau K, De Larochellière É, et al. Cardiac morphology and function reference values derived from a large subset of healthy young Caucasian adults by magnetic resonance imaging. *Eur Hear J – Cardiovasc Imag*. 2016;17:981–990.

2 van der Ven JPG, Sadighy Z, Valsangiacomo Buechel ER, et al. Multicentre reference values for cardiac magnetic resonance imaging derived ventricular size and function for children aged 0–18 years. *Eur Hear J - Cardiovasc Imag*. 2020;21:102–113.

3 Kanagala P, Arnold JR, Cheng ASH, et al. Left atrial ejection fraction and outcomes in heart failure with preserved ejection fraction. *Int J Cardiovasc Imag*. 2020;36:101–110.

4 Ferreira VM, Schulz-Menger J, Holmvang G, et al. Cardiovascular magnetic resonance in nonischemic myocardial inflammation. *J Am Coll Cardiol*. 2018;72:3158–3176.

5 Messroghli DR, Moon JC, Ferreira VM, et al. Clinical recommendations for cardiovascular magnetic resonance mapping of T1, T2, T2* and extracellular volume: a consensus statement by the Society for Cardiovascular Magnetic Resonance (SCMR) endorsed by the European Association for Cardiovascular Imagi. *J Cardiovasc Magn Reson*. 2017;19:75.

6 Buechel EV, Kaiser T, Jackson C, Schmitz A, Kellenberger CJ. Normal right- and left ventricular volumes and myocardial mass in children measured by steady state free precession cardiovascular magnetic resonance. *J Cardiovasc Magn Reson*. 2009;11:19.

7 Robbers-Visser D, Boersma E, Helbing WA. Normal biventricular function, volumes, and mass in children aged 8 to 17 Years. *J Magn Reson Imag*. 2009;29:552–559.

8 Sarikouch S, Peters B, Gutberlet M, et al. Sex-specific pediatric percentiles for ventricular size and mass as reference values for cardiac MRI. *Circ Cardiovasc Imag*. 2010;3:65–76.

9 Sarikouch S, Koerperich H, Boethig D, et al. Reference values for atrial size and function in children and young adults by cardiac MR: a study of the German competence network congenital heart defects. *J Magn Reson Imag*. 2011;33:1028–1039.

10 Fernandez-Jimenez R, Santos-Beneit G, Tresserra-Rimbau A, et al. Rationale and design of the school-based SI! Program to face obesity and promote health among Spanish adolescents: a cluster-randomized controlled trial. *Am Heart J*. 2019;215:27–40.

11 Fernandez-Jimenez R, Santos-Beneit G, de Cos-Gandoy A, et al. Prevalence and correlates of cardiovascular health among early adolescents enrolled in the SI! Program in Spain: a cross-sectional analysis. *Eur J Prev Cardiol*. 2022:29.e7–10.

12 von Elm E, Altman DG, Egger M, et al. The Strengthening the Reporting of Observational Studies in Epidemiology (STROBE) statement: guidelines for reporting observational studies. *Lancet (London, England)*. 2007;370:1453–1457.

13 Fernández-Jiménez R, Sánchez-González J, Aguero J, et al. Fast T2 gradient-spin-echo (T2-GraSE) mapping for myocardial edema quantification: first in vivo validation in a porcine model of ischemia/reperfusion. *J Cardiovasc Magn Reson*. 2015;17:92.

14 Fryar CD, Carroll MD, Gu Q, Afful J, Ogden CL. Anthropometric reference data for children and adults: United States, 2015-2018. *Vital Health Statistics - Ser 3 Anal Epidemiol Stud*. 2021:1–44.

15 Peters DC, Lamy J, Sinusas AJ, Baldassarre LA. Left atrial evaluation by cardiovascular magnetic resonance: sensitive and unique biomarkers. *Eur Hear J - Cardiovasc Imag*. 2021;23:14–30.

16 Alfuhied A, Marrow BA, Elfawal S, et al. Reproducibility of left atrial function using cardiac magnetic resonance imaging. *Eur Radiol*. 2021;31:2788–2797.

17 Cerqueira MD, Weissman NJ, Dilsizian V, et al. Standardized myocardial segmentation and nomenclature for tomographic imaging of the heart. *Circulation*. 2002;105:539–542.

18 Schulz-Menger J, Bluemke DA, Bremerich J, et al. Standardized image interpretation and post-processing in cardiovascular magnetic resonance - 2020 update. *J Cardiovasc Magn Reson*. 2020;22:19.

19 Dorfman AL, Geva T, Samyn MM, et al. SCMR expert consensus statement for cardiovascular magnetic resonance of acquired and non-structural pediatric heart disease. *J Cardiovasc Magn Reson*. 2022;24:44.

20 Radbruch A, Paech D, Gassenmaier S, et al. 1.5 vs 3 Tesla magnetic resonance imaging. *Invest Radiol*. 2021;56:692–704.

21 Petersen SE, Aung N, Sanghvi MM, et al. Reference ranges for cardiac structure and function using cardiovascular magnetic resonance (CMR) in Caucasians from the UK Biobank population cohort. *J Cardiovasc Magn Reson*. 2017;19:18.

22 Kawel-Boehm N, Hetzel SJ, Ambale-Venkatesh B, et al. Reference ranges ("normal values") for cardiovascular magnetic resonance (CMR) in adults and children: 2020 update. *J Cardiovasc Magn Reson*. 2020;22:87.

23 Aquaro GD, Camastra G, Monti L, et al. Reference values of cardiac volumes, dimensions, and new functional parameters by MR: a multicenter, multivendor study. *J Magn Reson Imag*. 2017;45:1055–1067.

24 Yeon SB, Salton CJ, Gona P, et al. Impact of age, sex, and indexation method on MR left ventricular reference values in the framingham heart study offspring cohort. *J Magn Reson Imag*. 2015;41:1038–1045.

25 Gandy SJ, Lambert M, Belch J, et al. 3T MRI investigation of cardiac left ventricular structure and function in a UK population: the tayside screening for the prevention of cardiac events (TASC-FORCE) study. *J Magn Reson Imag*. 2016;44:1186–1196.

26 Hoit BD. Left atrial size and function. *J Am Coll Cardiol*. 2014;63:493–505.

27 Gao Y, Zhang Z, Zhou S, et al. Reference values of left and right atrial volumes and phasic function based on a large sample of healthy Chinese adults: a cardiovascular magnetic resonance study. *Int J Cardiol*. 2022;352:180–187.

28 Maceira AM, Cosin-Sales J, Prasad SK, Pennell DJ. Characterization of left and right atrial function in healthy volunteers by cardiovascular magnetic resonance. *J Cardiovasc Magn Reson*. 2016;18:64.

29 Linden K, Goldschmidt F, Laser KT, et al. Left atrial volumes and phasic function in healthy children: reference values using real-time three-dimensional echocardiography. *J Am Soc Echocardiogr*. 2019;32:1036–1045.e9.

30 Panesar DK, Burch M. Assessment of diastolic function in congenital heart disease. *Front Cardiovasc Med*. 2017;4. https://doi.org/10.3389/fcvm.2017.00005.

31 Ta HT, Alsaied T, Steele JM, et al. Atrial function and its role in the non-invasive evaluation of diastolic function in congenital heart disease. *Pediatr Cardiol*. 2020;41:654–668.

32 Gottbrecht M, Kramer CM, Salerno M. Native T1 and extracellular volume measurements by cardiac MRI in healthy adults: a meta-analysis. *Radiology*. 2019;290:317–326.

33 Kellman P, Hansen MS. T1-mapping in the heart: accuracy and precision. *J Cardiovasc Magn Reson*. 2014;16:2.

34 Piechnik SK, Ferreira VM, Lewandowski AJ, et al. Normal variation of magnetic resonance T1 relaxation times in the human population at 1.5 T using ShMOLLI. *J Cardiovasc Magn Reson*. 2013;15:13.

35 Roy C, Slimani A, de Meester C, et al. Age and sex corrected normal reference values of T1, T2 T2* and ECV in healthy subjects at 3T CMR. *J Cardiovasc Magn Reson*. 2017;19:72.